Published in final edited form as:
Invest Ophthalmol Vis Sci. ; 54(5): 3569–3578. doi:10.1167/iovs.12-11125.

A CNS-Specific Hypomorphic Pdgfr-Beta Mutant Model of Diabetic Retinopathy

Shalini Jadeja[1], **Richard L. Mort**[1], **Margaret Keighren**[1], **Alan W. Hart**[1], **Russell Joynson**[2], **Sara Wells**[2], **Paul K. Potter**[2], and **Ian J. Jackson**[1,*]

[1]MRC Human Genetics Unit, MRC Institute of Genetics & Molecular Medicine, University of Edinburgh, Edinburgh, UK

[2]MRC Harwell, Oxfordshire, UK

Abstract

Purpose—A mouse mutant identified during a recessive ENU mutagenesis screen exhibited ocular haemorrhaging resulting in a blood filled orbit, and hence was named '*redeye*'. We aimed to identify the causal mutation in *redeye*, and evaluate it as a model for Diabetic Retinopathy (DR).

Methods—The causative gene mutation in *redeye* was identified by haplotype mapping followed by exome sequencing. Glucose tolerance tests, detailed histological and immunofluorescence analyses, and vascular permeability assays were performed to determine the affect of *redeye* on glucose metabolism, pericyte recruitment and the development of the retinal vasculature and the blood retinal barrier (BRB).

Results—A mutation was identified in the *Pdgfrb* gene at position +2 of intron 6. We show that this change causes partial loss of normal splicing resulting in a frameshift and premature termination, and therefore a substantial reduction in normal *Pdgfrb* transcript. The animals exhibit defective pericyte recruitment restricted to the central nervous system (CNS) causing basement membrane and vascular patterning defects, impaired vascular permeability and aberrant BRB development, resulting in vascular leakage and retinal ganglion cell apoptosis. Despite exhibiting classical features of diabetic retinopathy *redeye* glucose tolerance is normal.

Conclusions—The $Pdgfrb^{redeye/redeye}$ mice exhibit all of the features of non-proliferative DR including retinal neurodegeneration. In addition, the perinatal onset of the CNS-specific vascular phenotype negates the need to age animals or manage diabetic complications in other organs. Therefore they are a more useful model for diseases involving pericyte deficiencies such as DR than those currently being used.

INTRODUCTION

Platelet derived growth factors (Pdgfs) are powerful mitogens and important regulators of embryological development, cell proliferation, migration and survival. First described [1, 2], as

[*]**CORRESPONDING AUTHOR**: Telephone: +44 (0)131 467 8409 ian.jackson@igmm.ed.ac.uk.
DISCLOSURES/DISCLAIMERS: None

Europe PMC Funders Author Manuscripts

stimulating cell growth and proliferation, Pdgfs have two chains, A and B. Their receptors Pdgfrα and Pdgfrβ are transmembrane tyrosine kinases [3-7]. Pdgfrα is able to bind both PdgfA and B isoforms whereas Pdgfrβ can only bind PdgfB with high affinity [4, 5].

Pericytes are perivascular cells located on the abluminal surface of endothelial cells and are embedded within the basement membrane [8]. PdgfB is secreted by endothelial tip cells at the front of the extending vessel, which recruits Pdgfrβ-expressing mural cells such as vascular smooth muscle cells and pericytes to developing blood vessels during angiogenesis [9, 10]. These mural cells play an important role in the remodelling and stabilisation of blood vessels [11, 12].

The functions of pericytes include roles in vascular development, immune and phagocytic functions and haemostasis (reviewed in [8, 13]). More recently, pericytes have been shown to induce the formation of tight junctions between central nervous system (CNS) endothelial cells to form the blood brain barrier (BBB) and blood retinal barrier (BRB) [14, 15].

PdgfB/Pdgfrβ signalling is crucial for pericyte recruitment and survival [16], with mutations in these molecules resulting in pericyte recruitment deficiencies [12]. PdgfRβ null mice are usually lethal due to severe haemorrhaging either in utero or at birth [17], however mice harbouring specific mutations in Pdgfrβ are viable [18, 19].

A major complication of diabetes mellitus is diabetic retinopathy (DR) which is one of the leading causes of blindness worldwide. DR is characterised by ‘pericyte drop-out’ which has severe irreversible pathological consequences for the retina characterised by microvascular abnormalities such as endothelial dysfunction and haemorrhage, and neuronal abnormalities including retinal ganglion cell (RGC) death [20, 21]. Prolonged hyperglycemia in the retina activates PKC-δ and SHP-1 inhibiting Pdgfrβ signalling resulting in pericyte apoptosis [22]. Some of the features of DR have also been identified in mice with diminished Pdgfrβ signalling [23-25], indeed PdgfB has been implicated in DR for many years [26].

Here we present a mouse mutant, *redeye*, with decreased pericyte coverage in the CNS caused by an *N*-ethyl-*N*-nitrosourea (ENU)-induced mutation in *Pdgfrb*. Most other DR mouse models currently in use do not exhibit all of the features of DR, namely pericyte and RGC loss, BRB breakdown, vascular leakage, and acellular capillaries [20, 27-31]. The *redeye* strain exhibits all the features of DR within weeks of birth, negating the need to age experimental animals and without the multiple organ involvement [12, 16, 18, 23, 24, 26, 32-34] seen in other PdgfB/Pdgfrβ mutants. This enables easier isolation of the vascular defects in the *redeye* mice and makes them a less complicated disease model. Of particular note is that this strain and DR have the same underlying cause for pericyte loss, as hyperglycemia can result in decreased signalling from Pdgfrβ causing subsequent pericyte apoptosis [22]. Furthermore, the defect in BRB development makes them a useful tool for dissecting the role of pericytes in BRB formation and vascular development.

MATERIALS AND METHODS

Experimental animals

The *redeye* strain, referred to as *Pdgfrb*^{redeye} in this manuscript, was maintained on a sighted C3H background [35]. The following primers were used for sequencing for genotyping. 5′-CATTGTGATGGGCAATGATG-3′ and 5′-ATAGGTGCCCGAATCACTCA-3′. All experiments complied with the ARVO Statement for the Use of Animals in Ophthalmic and Vision Research and the relevant local animal welfare conditions.

Mutation identification

Initial mapping by SNP array analysis (University of Edinburgh, Wellcome Trust Clinical Research Facility) identified an 8 Mb region of interest. All exons and splice junctions in this region were captured on a custom oligonucleotide-array, amplified and sequenced, identifying a mutation in the *Pdgfrb* gene which was confirmed by Sanger sequencing. To characterise the mutation we extracted RNA from enucleated eyes and performed quantitative real-time PCR using the Mouse Universal ProbeLibrary Set (Roche, UK) with probes for Pdgfrβ and TBP on a Roche Lightcycler LC480. The Lightcycler LC480 software was used to normalise results to TBP controls and calculate relative expression values.

Tissue preparation and Immunofluorescence

Mice were sacrificed at the appropriate age and wholemount retinae were prepared and stained as described [36]. We stained mutant and control retinae in the same well to control for changes in staining efficiency, retinae were distinguished by different numbers of radial incisions.

Embryonic hindbrains were dissected as previously described [37] and all other organs were dissected from animals of the appropriate age and fixed in 4% PFA overnight at 4°C. Postnatal day 5 (P5) brains were embedded in 4% agarose in PBS and 200 μm sections were cut on a Vibratome Series 1000 (Technical Products International Inc). Immunofluorescence for hindbrains and brain sections was performed as for retinae.

We embedded the kidneys in paraffin for sectioning on a Leica RM 2235 microtome. Placentae and hearts were cryopreserved in 30% sucrose and embedded in OCT compound (VWR International, UK) for sectioning on a Leica CM30505 cryostat. Citrate buffer antigen retrieval was used for paraffin sections. We blocked all the sections in 10% heat inactivated donkey serum in PBST for an hour, and performed all antibody incubations at room temperature for an hour in block (antibody details are given in Supp Table S1). Haematoxylin and Eosin staining were performed according to standard procedures.

Tissue from at least five mice of each genotype from at least three different litters was used for all analysis. All tissues were mounted in Vectashield (Vector Laboratories, UK), imaged by confocal microscopy (Nikon A1R) and maximum intensity projections of z-stacks were created using NisElements AR Version 4.0 software. All images are representative of at least three animals.

Immunoblot

We extracted protein from all tissues using 1xRIPA buffer (Cell Signaling Technology, USA) containing protease and phosphatase inhibitors (Roche, UK) and followed manufacturer's instructions. The NuPage gel electrophoresis and XCell II blotting systems (Invitrogen, UK) were used for protein separation and immunoblotting respectively. Blots were blocked in 5% milk/TBST and all antibodies (details given in Supp. Table S2) were incubated in block for 1 hour at room temperature. Immunolabelling was detected using the Amersham ECL plus Western blotting kit (GE Healthcare, UK). Quantification was performed using ImageQuant TL software.

Pericyte and Branchpoint Quantification

The MetaMorph® Angiogenesis Tube Formation application (Molecular Devices, UK) was used for quantification. Confocal images were used to determine the total area covered by vessels and pericytes in order to calculate percentage pericyte coverage of vessels and the total number of branchpoints/mm^2. We imaged three areas of each retina; three different regions of the central retina each encompassing an artery and vein, and two images each of peripheral arteries and peripheral veins; a total of five images/retina. For pericyte quantification of the cerebral cortex capillaries, sections from the frontal, parietal and occipital regions of the brain were used and four images were taken from the cerebral cortex of each section. Threshold values were kept the same for analysis of samples of the same stage.

Avascular region measurement

As a measure of vascular branching we counted the number and area of the avascular regions between capillaries for each image, again for the three regions of each retina. Image analysis was performed using a custom macro written for the freeware image analysis package Fiji [38] which is based on ImageJ [39]. The macro requires Gabriel Landini's 'Morphological Operators for ImageJ' available from http://www.dentistry.bham.ac.uk/landinig/software/software.html.

Permeability assay

Fluorescence angiography was performed as previously described [40] with modifications. Mice were injected intraperitoneally at P10 with 40 μl of 50 mg/ml Fitc conjugated Dextran 20000S (Sigma, UK) w/v in PBS, sacrificed an hour later, the retinae dissected and imaged using a Zeiss Axioplan II fluorescence microscope and a Coolsnap HQ CCD camera (Photometrics Ltd, Tucson, AZ). IPLab Spectrum software (Scanalytics Corp, Fairfax, VA) was used to analyse retinal haemorrhages.

Retinal Ganglion Cell and Macrophage count

Volocity 3D Image analysis software (PerkinElmer) was used for both RGC and macrophage counts. Cells positively stained for the RGC marker Brn3 were counted in the centre of fully mature retinae (P28), which our preliminary data (not shown) suggested was the region most affected in our mutants.

Statistical Analysis

Statistical tests were performed using the 'R' statistics package, an open source software package based on the 'S' programming language (http://www.R-project.org). The appropriate parametric or non-parametric tests used are detailed in Supp. Table S3.

Glucose Tolerance Tests

Eight week old animals were fasted for five hours prior to intraperitoneal injection of 2 g glucose (Sigma, UK) per kilogram of body weight. Blood was drawn from the tail vein at 0, 30, 60, 90, and 120 minutes after injection and glucose values were monitored using an automatic glucometer (Accuchek, Roche, UK). Numbers of mice tested are females (4 WT, 6 Hom) and males (6 WT, 5 Hom).

RESULTS

redeye is a hypomorphic mutation in *Pdgfrb*

The *redeye* strain was identified during an ENU-induced mutagenesis screen for recessive eye mutations at MRC Harwell and initially presented with severe haemorrhaging in the eye (not shown). The severity of the haemorrhaging was reduced upon crossing the strain onto a congenic C3H strain lacking the *Pde6b*^{rd1} mutation [35]. Mutants show normal responses during optokinetic response drum testing (data not shown). No further defects were identified during phenotyping at MRC Harwell and the *redeye* mice have a normal lifespan.

We identified a T to C mutation in the *Pdgfrb* gene, encoding Pdgfrβ, affecting the splice donor site at position +2 of intron 6 changing the consensus GT to the less efficiently utilised GC [41]. To investigate the impact of this change on splicing we extracted RNA from P5 eyes and performed RT-PCR. In addition to the PCR product from the normally spliced transcript, we detected a product of increased size in homozygotes, sequencing of which confirmed the retention of intron 6 (Fig. 1A, B) in mutant mRNA. This additional sequence introduces 23 novel amino acids followed by premature termination. The normally spliced *Pdgfrb* transcript was present but quantitative RT-PCR showed that mutant eyes contain only approximately 25% of wildtype levels of *Pdgfrb* mRNA (Fig. 1C). This corresponds to a decrease in Pdgfrβ protein seen by immunoblotting and immunofluorescence of homozygote retinae (Fig. 1D, 2) confirming *Pdgfrb*^{redeye} is a hypomorphic mutant allele of *Pdgfrb*.

The *redeye* mutation causes decreased pericyte coverage restricted to the CNS

Pdgfrβ is required for pericyte recruitment so we performed immunofluorescence on perinatal wholemount retinae to determine whether decreased Pdgfrβ caused a corresponding decrease in pericyte coverage. As there is no definitive marker of pericytes a panel of markers is required to correctly identify these cells [42]. This confirmed a decrease in pericytes as shown by a reduction in Pdgfrβ (Fig. 2G), alpha smooth muscle actin (Fig. 2H), proteoglycan NG2 (Fig. 2J), endosialin and desmin (Supp. Fig. S1). We found that proteoglycan NG2 (NG2) is the most robust of these markers in the mouse retina and therefore used it as a specific pericyte marker for our further investigations in the retina.

In order to quantify this reduction in pericytes, we stained wholemount retinae for NG2 to mark pericytes and isolectin B4 (IB4) to mark the endothelium. We analysed retinae at P5, when the primary vascular plexus has grown halfway between the optic nerve head and the periphery of the retina, and at P10 when the primary vascular plexus is fully mature. There is a significant decrease in pericyte coverage in all three retinal regions (central, peripheral vein and peripheral artery) in *Pdgfrb*$^{redeye/redeye}$ vs wildtype animals at P5 and P10 (Fig. 2K, L).

Other *Pdgfrb* mutants have defects in the recruitment of mesangial cells [26], the pericyte equivalent in the kidney, with subsequent developmental defects. We therefore harvested kidneys at embryonic day 17.5 (E17.5) when mesangial cells begin to invade the kidney glomerulus. Staining for podocytes and mesangial cells showed no apparent defect in mesangial cell recruitment (Fig. 3A-C, E-G). We also analysed adult *Pdgfrb*$^{redeye/redeye}$ kidneys which showed no histological defects (Fig. 3 D, H). Next we examined E18.5 placentae and hearts for the developmental abnormalities exhibited in other Pdgfrβ signalling mutants at this stage [23], and to determine whether pericyte recruitment was affected in these tissues. Our results show that both pericyte recruitment and histology of the embryonic heart and placenta are normal (Supp. Fig. S2), suggesting that the defect in pericyte coverage may be restricted to the CNS.

To test this we studied another model of angiogenesis, the mouse hindbrain, which is vascularised between E9.5 and E12.5. Flatmounted E12.5 hindbrains from *Pdgfrb*$^{redeye/redeye}$ mutants showed reduced NG2 staining (Fig. 3L-N). We then examined pericyte coverage of cerebral vessels in P5 animals. As NG2 stains oligodendricytes as well as pericytes in the brain we used desmin as a marker for pericytes (Supp. Fig. S3A-F). Repeated analysis of P5 retinae with desmin staining showed pericyte coverage similar to that obtained with NG2 staining (Supp. Fig. S3G). We found a statistically significant decrease in pericyte coverage in *Pdgfrb*$^{redeye/redeye}$ mutants in the cerebral cortex (Supp. Fig. S3G) confirming that the reduction in pericyte coverage was widespread in, but limited to the CNS.

The *Pdgfrb*$^{redeye/redeye}$ mice exhibit basement membrane deposition and vascular patterning defects

During this analysis we noted that there was a defect in vessel patterning (Fig. 4A, D), with increased vessel tortuousity in the mutants (Fig. 4E). Pericytes secrete their own basement membrane, so a reduction in pericytes would likely result in decreased basement membrane coverage. Immunofluorescence on the mutant retinae indeed shows less collagen IV coverage of the vessels with additional weaker expression on perivascular cells, which may be pericytes that have failed to adhere due to reduced Pdgfrβ signalling (Fig. 4C, F). Furthermore, artery-vein crossover events (Fig. 4I) and acellular capillaries or ‘ghost vessels’, (Fig. 4J) are present in mutant retinae.

Analysis of *Pdgfrb*$^{redeye/redeye}$ retinae also revealed a defect in vessel branching (Fig. 5). To quantify this we used image analysis software to count the number of avascular regions in each image (Fig. 5A-D) which showed a significant decrease in the number of these regions

in the *Pdgfrb*$^{redeye/redeye}$ animals (Fig. 5E). There is also a significant reduction in the number of branchpoints in *Pdgfrb*$^{redeye/redeye}$ animals (Fig. 5F).

Vascular permeability and Blood Retinal Barrier development are impaired in *Pdgfrb*$^{redeye/redeye}$ mice

Initial phenotyping had shown ocular haemorrhage, consequently we investigated the vascular leakage further by using fluorescently labelled 2 kDa dextran which should not pass through the BRB. We found leakage from *Pdgfrb*$^{redeye/redeye}$ retinal vessels into the vitreous within an hour of injection (Fig. 6D). No haemorrhage or leakage was observed in control organs e.g. kidney (not shown) or in the retinae of wildtype mice (Fig. 6A). As pericytes have been linked to BRB induction[14, 15], we next looked at the expression of BRB markers. The tight junction molecules claudin 5 and zona occludens 1 (ZO1) are expressed in both mutant and control retinae (Fig. 6B, C, E, F). BRB dysfunction can cause neurodegeneration, therefore we counted RGCs in the *Pdgfrb*^{redeye} mice (Fig. 6H, K). Our results show that there is a significant decrease in the number of RGCs in the central retina of *Pdgfrb*$^{redeye/redeye}$ animals, relative to wildtypes by P28 (Fig. 6H, K, M). This is due to RGC apoptosis as seen by positive cleaved caspase 3 staining (Fig. 6I, L), confirming neurodegeneration in the *Pdgfrb*$^{redeye/redeye}$ mutants.

The *Pdgfrb*$^{redeye/redeye}$ mice have normal glucose tolerance

The features we describe in *Pdgfrb*$^{redeye/redeye}$ mice are symptomatic of DR, including decreased pericyte coverage, increased vascular permeability and BRB loss. It is therefore important to exclude diabetes as the cause of this retinopathy. We performed glucose tolerance tests which show that the *Pdgfrb*$^{redeye/redeye}$ mice were able to clear injected glucose (Supp. Fig. S4). The mutants also express insulin and glucagon at wildtype levels (not shown) and are therefore not diabetic.

DISCUSSION

redeye mutants exhibit a CNS-specific reduction in pericytes

Pdgfrb^{redeye} is a *Pdgfrb* partial loss of function mutant expressing approximately 58% of the wildtype levels of Pdgfrβ. Much work has previously shown the requirement of Pdgfrβ signalling for the recruitment of pericytes to the developing vasculature [9, 10, 17, 18, 33, 37, 43-45]. We confirm that a reduction in Pdgfrβ results in decreased pericyte coverage in retinae at P5 and P10 (Fig. 2) due to its requirement for the initial expansion and propagation of pericytes.

Pdgfrb null mice die at/shortly after birth from severe haemorrhaging due to pericyte deficiency [16-18]. However, the *Pdgfrb*$^{redeye/redeye}$ mice are viable and occur at Mendelian ratios (not shown) with only the CNS vasculature exhibiting a reduction in pericytes (Fig. 2, 3, Supp. Fig. S1-S3). Previous reports describe similar variations in pericyte deficiency between different organs in other *Pdgfrb* mutants [13]. This could be due to Pdgfrα compensating for the loss of Pdgfrβ in these tissues [18]. However, our data shows that Pdgfrα is not upregulated in the retina in response to decreased Pdgfrβ expression (Supp. Fig. S1). It is more likely that the CNS-restricted phenotype is due to the higher

pericyte:endothelial cell ratio in the CNS which is as high as 1:3 in the brain, compared with 1:100 in striated muscle, and is reportedly even higher in the retina [46, 47]. Our results support previous findings that even within the CNS, pericyte coverage of capillaries can vary [48]. We found approximately 40% of vessels are covered by pericytes in wildtype P5 cerebral cortex compared to approximately 80% coverage in the wildtype retina (Supp. Fig. S3G).

This increased pericyte density results in higher expression of Pdgfrβ in wildtype adult CNS tissues. Pdgfrβ expression in the brain is much higher than in other organs with a dramatic decrease in the expression of Pdgfrβ in *Pdgfrb*$^{redeye/redeye}$ mutants in the CNS (Supp. Fig. S5). Interestingly, Pdgfrβ is expressed at the same level in *Pdgfrb*$^{redeye/redeye}$ mutant and wildtype kidneys (Supp. Fig. S5A), which may explain why *Pdgfrb*$^{redeye/redeye}$ kidneys are unaffected. The reduced expression of Pdgfrβ in the *Pdgfrb*$^{redeye/redeye}$ hypomorphs may be sufficient to support a subpopulation of pericytes that are less sensitive to decreased Pdgfrβ signalling and enable vascular function outside the CNS. Also, as pericytes have a specific role in BRB formation[14, 15] the CNS may be more sensitive to changes in Pdgfrβ.

Pericytes are crucial for vessel patterning and endothelial maturation

Our work confirms that a decrease in pericyte numbers affects vessel patterning. It has been established that during angiogenesis the initial vascular plexus is remodelled to form a fully functional vascular network [9, 49]. Pericytes prevent excessive remodelling by conferring vascular stability [11, 12, 49]. A delay or reduction in pericyte recruitment as seen in the *Pdgfrb*$^{redeye/redeye}$ mice would thus enable increased vascular pruning to occur resulting in a sparser vascular network with fewer branchpoints and fewer, but larger avascular regions between the vessels (Fig. 5). This further highlights the importance of pericytes during angiogenesis.

redeye mutants model Diabetic Retinopathy

Previous findings show that loss of pericytes in the CNS and the resultant vascular permeability is due to an increase in transcytosis [14]. We can confirm this in the *Pdgfrb*$^{redeye/redeye}$ mutants in which BRB dysfunction manifests as increased vascular permeability with normal tight junction formation (Fig. 6B, C, E, F). *Pdgfrb*$^{redeye/redeye}$ mutants also exhibit the classic DR features of acellular capillaries (Fig. 4J) and neurodegeneration in the form of a reduced number of RGCs (Fig. 6G-K), though pericyte ghosts are not seen. Acellular capillaries arise as a consequence of endothelial cell apoptosis due to the loss of pericyte-derived survival signals [50] or a loss of the BRB [51], leaving an acellular basement membrane (Fig. 4J). As is the case in diabetes, the remaining endothelium is oxidatively stressed and produces less neurotrophic factors [52], resulting in neurodegeneration (Fig. 6G-K). RGCs are particularly sensitive to retinal ischemia and neurotoxicity [53, 54] and are often damaged in ischemic retinopathies such as DR. RGC apoptosis is seen much later than the vascular defects and we conclude that vascular dysfunction preceeds neurodegeneration in this model. This is a particularly important finding given the controversy regarding whether diabetic mouse models exhibit RGC loss [20, 27, 55].

Europe PMC Funders Author Manuscripts

The early perinatal onset of these vascular changes is particularly useful as most other DR models currently in use do not exhibit vascular pathology until at least 8 weeks of age [27-31] and do not show the full range of vascular and neuronal defects exhibited in this model. Though the *Pdgfrb*^{redeye} mutants do not exhibit hyperglycaemia, they have the same cause for reduced pericytes i.e. diminished Pdgfrβ signalling, resulting in the same phenotype. As the *Pdgfrb*$^{redeye/redeye}$ mice do not exhibit neovascularisation we propose that the *Pdgfrb*^{redeye} strain is a useful model for non-proliferative DR. The insights gained by studying this mutant will not only be valuable for understanding how pericytes are involved in maintaining a normal retinal vasculature but also their role in BBB/BRB formation.

Supplementary Material

Refer to Web version on PubMed Central for supplementary material.

Acknowledgments

We would like to thank David Black and animal staff for animal husbandry, Matthew Pearson and Paul Perry for imaging assistance, Allyson Ross for histology assistance and Alexi Balmuth at the Genepool for exome sequencing. We are also grateful to Clare Isacke, BBCRC, London, UK for the kind gift of the anti-Endosialin antibody.

SUPPORT:

This research was supported by Eumodic; the European Mouse Disease Clinic, an EU Integrated Research Programme and MRC Core Support to the MRC Human Genetics Unit and the MRC Mammalian Genetics Unit.

REFERENCES

1. Kohler N, Lipton A. Platelets as a source of fibroblast growth-promoting activity. Exp Cell Res. 1974; 87:297–301. [PubMed: 4370268]
2. Ross R, Glomset J, Kariya B, Harker L. A platelet-dependent serum factor that stimulates the proliferation of arterial smooth muscle cells in vitro. Proc Natl Acad Sci U S A. 1974; 71:1207–1210. [PubMed: 4208546]
3. Gronwald RG, Grant FJ, Haldeman BA, et al. Cloning and expression of a cDNA coding for the human platelet-derived growth factor receptor: evidence for more than one receptor class. Proc Natl Acad Sci U S A. 1988; 85:3435–3439. [PubMed: 2835772]
4. Hart CE, Forstrom JW, Kelly JD, et al. Two classes of PDGF receptor recognize different isoforms of PDGF. Science. 1988; 240:1529–1531. [PubMed: 2836952]
5. Heldin CH, Backstrom G, Ostman A, et al. Binding of different dimeric forms of PDGF to human fibroblasts: evidence for two separate receptor types. Embo J. 1988; 7:1387–1393. [PubMed: 2842148]
6. Heldin CH, Hammacher A, Nister M, Westermark B. Structural and functional aspects of platelet-derived growth factor. Br J Cancer. 1988; 57:591–593. [PubMed: 2841963]
7. Matsui T, Heidaran M, Miki T, et al. Isolation of a novel receptor cDNA establishes the existence of two PDGF receptor genes. Science. 1989; 243:800–804. [PubMed: 2536956]
8. Allt G, Lawrenson JG. Pericytes: Cell Biology and Pathology. Cells Tissues Organs. 2001; 169:1–11. [PubMed: 11340256]
9. Fruttiger M. Development of the retinal vasculature. Angiogenesis. 2007; 10:77–88. [PubMed: 17322966]
10. Risau W. Mechanisms of angiogenesis. Nature. 1997; 386:671–674. [PubMed: 9109485]
11. Benjamin LE, Hemo I, Keshet E. A plasticity window for blood vessel remodelling is defined by pericyte coverage of the preformed endothelial network and is regulated by PDGF-B and VEGF. Development. 1998; 125:1591–1598. [PubMed: 9521897]

12. Lindahl P, Johansson BR, Leveen P, Betsholtz C. Pericyte Loss and Microaneurysm Formation in PDGF-B-Deficient Mice. Science. 1997; 277:242–245. [PubMed: 9211853]
13. Armulik A, GenovÃ© G, Betsholtz C. Pericytes: Developmental, Physiological, and Pathological Perspectives, Problems, and Promises. Developmental cell. 2011; 21:193–215. [PubMed: 21839917]
14. Armulik A, Genove G, Mae M, et al. Pericytes regulate the blood-brain barrier. Nature. 2010; 468:557–561. [PubMed: 20944627]
15. Daneman R, Zhou L, Kebede AA, Barres BA. Pericytes are required for blood-brain barrier integrity during embryogenesis. Nature. 2010; 468:562–566. [PubMed: 20944625]
16. Hoch RV, Soriano P. Roles of PDGF in animal development. Development. 2003; 130:4769–4784. [PubMed: 12952899]
17. Soriano P. Abnormal kidney development and hematological disorders in PDGF beta-receptor mutant mice. Genes Dev. 1994; 8:1888–1896. [PubMed: 7958864]
18. Tallquist MD, French WJ, Soriano P. Additive effects of PDGF receptor beta signaling pathways in vascular smooth muscle cell development. PLoS Biol. 2003; 1:E52. [PubMed: 14624252]
19. Winkler EA, Bell RD, Zlokovic BV. Pericyte-specific expression of PDGF beta receptor in mouse models with normal and deficient PDGF beta receptor signaling. Mol Neurodegener. 2011; 5:32. [PubMed: 20738866]
20. Robinson R, Barathi VA, Chaurasia SS, Wong TY, Kern TS. Update on animal models of diabetic retinopathy: from molecular approaches to mice and higher mammals. Disease Models & Mechanisms. 2012; 5:444–456. [PubMed: 22730475]
21. Cheung N, Mitchell P, Wong TY. Diabetic retinopathy. The Lancet. 2010; 376:124–136.
22. Geraldes P, Hiraoka-Yamamoto J, Matsumoto M, et al. Activation of PKC-[delta] and SHP-1 by hyperglycemia causes vascular cell apoptosis and diabetic retinopathy. Nat Med. 2009; 15:1298–1306. [PubMed: 19881493]
23. Bjarnegard M, Enge M, Norlin J, et al. Endothelium-specific ablation of PDGFB leads to pericyte loss and glomerular, cardiac and placental abnormalities. Development. 2004; 131:1847–1857. [PubMed: 15084468]
24. Enge M, Bjarnegard M, Gerhardt H, et al. Endothelium-specific platelet-derived growth factor-B ablation mimics diabetic retinopathy. Embo J. 2002; 21:4307–4316. [PubMed: 12169633]
25. Hammes H-P, Lin J, Renner O, et al. Pericytes and the Pathogenesis of Diabetic Retinopathy. Diabetes. 2002; 51:3107–3112. [PubMed: 12351455]
26. Lindblom P, Gerhardt H, Liebner S, et al. Endothelial PDGF-B retention is required for proper investment of pericytes in the microvessel wall. Genes Dev. 2003; 17:1835–1840. [PubMed: 12897053]
27. Barber AJ, Antonetti DA, Kern TS, et al. The Ins2Akita Mouse as a Model of Early Retinal Complications in Diabetes. Investigative Ophthalmology & Visual Science. 2005; 46:2210–2218. [PubMed: 15914643]
28. Cheung AKH, Fung MKL, Lo ACY, et al. Aldose Reductase Deficiency Prevents Diabetes-Induced Blood-Retinal Barrier Breakdown, Apoptosis, and Glial Reactivation in the Retina of db/db Mice. Diabetes. 2005; 54:3119–3125. [PubMed: 16249434]
29. Kador PF, Zhang P, Makita J, et al. Novel Diabetic Mouse Models as Tools for Investigating Diabetic Retinopathy. PLoS ONE. 2012; 7:e49422. [PubMed: 23251343]
30. Martin PM, Roon P, Van Ells TK, Ganapathy V, Smith SB. Death of Retinal Neurons in Streptozotocin-Induced Diabetic Mice. Investigative Ophthalmology & Visual Science. 2004; 45:3330–3336. [PubMed: 15326158]
31. Rakoczy EP, Rahman ISA, Binz N, et al. Characterization of a Mouse Model of Hyperglycemia and Retinal Neovascularization. The American Journal of Pathology. 2010; 177:2659–2670. [PubMed: 20829433]
32. Leveen P, Pekny M, Gebre-Medhin S, Swolin B, Larsson E, Betsholtz C. Mice deficient for PDGF B show renal, cardiovascular, and hematological abnormalities. Genes & Development. 1994; 8:1875–1887. [PubMed: 7958863]
33. Soriano P. The PDGF alpha receptor is required for neural crest cell development and for normal patterning of the somites. Development. 1997; 124:2691–2700. [PubMed: 9226440]

34. Uemura A, Ogawa M, Hirashima M, et al. Recombinant angiopoietin-1 restores higher-order architecture of growing blood vessels in mice in the absence of mural cells. The Journal of Clinical Investigation. 2002; 110:1619–1628. [PubMed: 12464667]
35. Hart AW, McKie L, Morgan JE, et al. Genotype-phenotype correlation of mouse pde6b mutations. Invest Ophthalmol Vis Sci. 2005; 46:3443–3450. [PubMed: 16123450]
36. West H, Richardson WD, Fruttiger M. Stabilization of the retinal vascular network by reciprocal feedback between blood vessels and astrocytes. Development. 2005; 132:1855–1862. [PubMed: 15790963]
37. Gerhardt H, Ruhrberg C, Abramsson A, Fujisawa H, Shima D, Betsholtz C. Neuropilin-1 is required for endothelial tip cell guidance in the developing central nervous system. Developmental Dynamics. 2004; 231:503–509. [PubMed: 15376331]
38. Schindelin J, Arganda-Carreras I, Frise E, et al. Fiji: an open-source platform for biological-image analysis. Nat Meth. 2012; 9:676–682.
39. Schneider CA, Rasband WS, Eliceiri KW. NIH Image to ImageJ: 25 years of image analysis. Nat Meth. 2012; 9:671–675.
40. Ramirez M, Wu Z, Moreno-Carranza B, et al. Vasoinhibin Gene Transfer by Adenoassociated Virus Type 2 Protects against VEGF- and Diabetes-Induced Retinal Vasopermeability. Investigative Ophthalmology & Visual Science. 2011; 52:8944–8950. [PubMed: 22003113]
41. Sheth N, Roca X, Hastings ML, Roeder T, Krainer AR, Sachidanandam R. Comprehensive splice-site analysis using comparative genomics. Nucleic Acids Res. 2006; 34:3955–3967. [PubMed: 16914448]
42. Ehler E, Karlhuber G, Bauer HC, Draeger A. Heterogeneity of smooth muscle-associated proteins in mammalian brain microvasculature. Cell Tissue Res. 1995; 279:393–403. [PubMed: 7895277]
43. Hellstrom M, Kaln M, Lindahl P, Abramsson A, Betsholtz C. Role of PDGF-B and PDGFR-beta in recruitment of vascular smooth muscle cells and pericytes during embryonic blood vessel formation in the mouse. Development. 1999; 126:3047–3055. [PubMed: 10375497]
44. Klinghoffer RA, Mueting-Nelsen PF, Faerman A, Shani M, Soriano P. The two PDGF receptors maintain conserved signaling in vivo despite divergent embryological functions. Mol Cell. 2001; 7:343–354. [PubMed: 11239463]
45. Lindahl P, Hellstrom M, Kalen M, et al. Paracrine PDGF-B/PDGF-Rbeta signaling controls mesangial cell development in kidney glomeruli. Development. 1998; 125:3313–3322. [PubMed: 9693135]
46. Dalkara T, Gursoy-Ozdemir Y, Yemisci M. Brain microvascular pericytes in health and disease. Acta Neuropathol. 2011; 122:1–9. [PubMed: 21656168]
47. Stewart PA, Tuor UI. Blood-eye barriers in the rat: correlation of ultrastructure with function. J Comp Neurol. 1994; 340:566–576. [PubMed: 8006217]
48. Frank RN, Turczyn TJ, Das A. Pericyte coverage of retinal and cerebral capillaries. Investigative Ophthalmology & Visual Science. 1990; 31:999–1007. [PubMed: 2354923]
49. Ribatti D, Crivellato E. 'Sprouting angiogenesis', a reappraisal. Developmental Biology. 2012; 372:157–165. [PubMed: 23031691]
50. Franco M, Roswall P, Cortez E, Hanahan D, Pietras K. Pericytes promote endothelial cell survival through induction of autocrine VEGF-A signaling and Bcl-w expression. Blood. 2011; 118:2906–2917. [PubMed: 21778339]
51. Barber AJ, Gardner TW, Abcouwer SF. The Significance of Vascular and Neural Apoptosis to the Pathology of Diabetic Retinopathy. Investigative Ophthalmology & Visual Science. 2011; 52:1156–1163. [PubMed: 21357409]
52. Navaratna D, Guo SZ, Hayakawa K, Wang X, Gerhardinger C, Lo EH. Decreased cerebrovascular brain-derived neurotrophic factor-mediated neuroprotection in the diabetic brain. Diabetes. 2011; 60:1789–1796. [PubMed: 21562076]
53. Vidal-Sanz M, Lafuente M, Sobrado-Calvo P, et al. Death and neuroprotection of retinal ganglion cells after different types of injury. Neurotox Res. 2000; 2:215–227. [PubMed: 16787842]
54. Yang Y, Mao D, Chen X, et al. Decrease in retinal neuronal cells in streptozotocin-induced diabetic mice. Mol Vis. 2012; 18:1411–1420. [PubMed: 22690119]

55. Feit-Leichman RA, Kinouchi R, Takeda M, et al. Vascular Damage in a Mouse Model of Diabetic Retinopathy: Relation to Neuronal and Glial Changes. Investigative Ophthalmology & Visual Science. 2005; 46:4281–4287. [PubMed: 16249509]

Europe PMC Funders Author Manuscripts

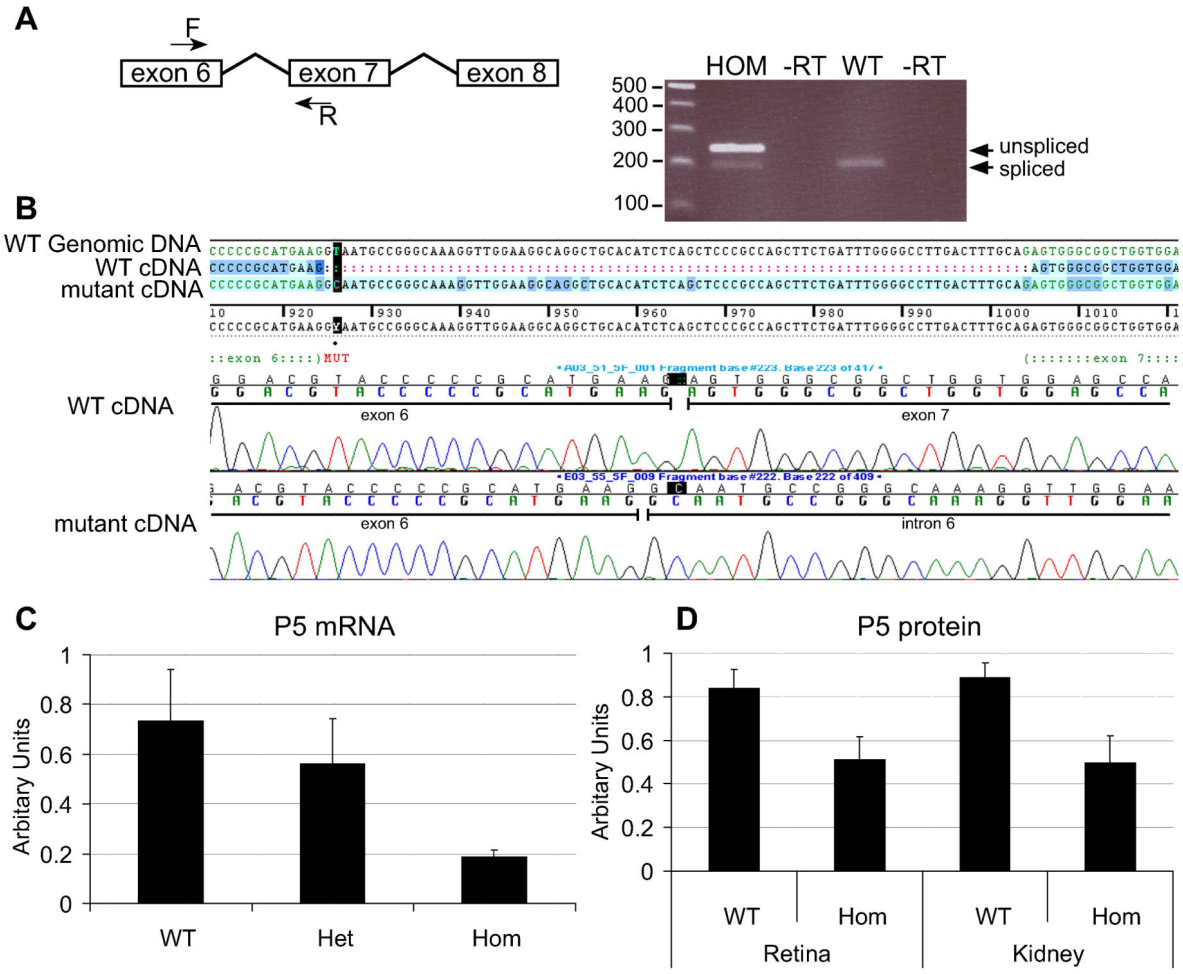

Figure 1. *redeye* is a hypomorphic mutant of *Pdgfrb*

A donor splice site mutation was identified in intron 6 of *Pdgfrb*, causing reduced splicing of the intron. RT-PCR between exons 6 and 7 results in a larger, unspliced RT-PCR product in homoygote animals (HOM) of 243 bp as well as the normally spliced product of 190 bp (A). Sequencing of these RT-PCR products shows that the mutant transcript contains intron 6 whereas the WT transcript does not (B). Quantitative analysis shows a decrease in *Pdgfrb* mRNA by quantitative RT-PCR (C) and protein by immunoblot (D). Error bars: standard deviation of the mean.

Europe PMC Funders Author Manuscripts

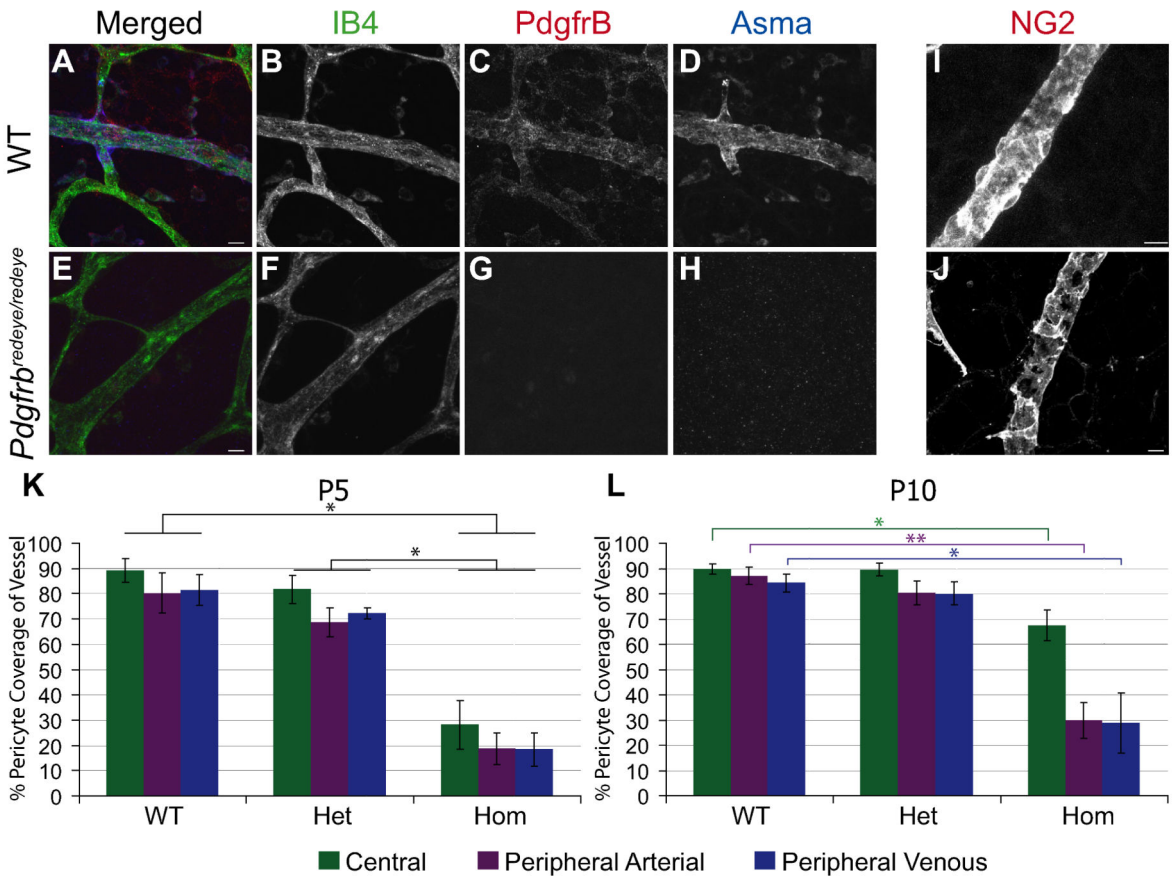

Figure 2. *Pdgfrb*$^{redeye/redeye}$ mutants have reduced pericyte coverage in the retina

Representative images of P5 retinal vasculature from WT (A-D) and *Pdgfrb*$^{redeye/redeye}$ mice (E-H). Vessels are stained with Isolectin B4 (IB4) and pericytes with Pdgfrβ (C) and Alpha smooth muscle actin (Asma) (D). Staining is not detected in *Pdgfrb*$^{redeye/redeye}$ mice (G, H). Another marker of pericytes, Proteoglycan NG2 (NG2) was also used on P5 retinae which gives more robust staining. Wildtype vessels (I) have more complete coverage by pericytes than mutant vessels (J). IB4 and NG2 stained retinae were used to quantify the percentage of the vessel covered by pericytes. Perictye coverage in *Pdgfrb*$^{redeye/redeye}$ (Hom) is significantly lower than both WT and *Pdgfrb*$^{redeye/+}$ (Het) at P5 and P10 (SRH test $P < 0.001$, Mann-Whitney U-test $*P < 0.05$, $**P < 0.005$) (K-L). All scale bars:10 μm. Error bars: standard deviation of the mean.

Europe PMC Funders Author Manuscripts

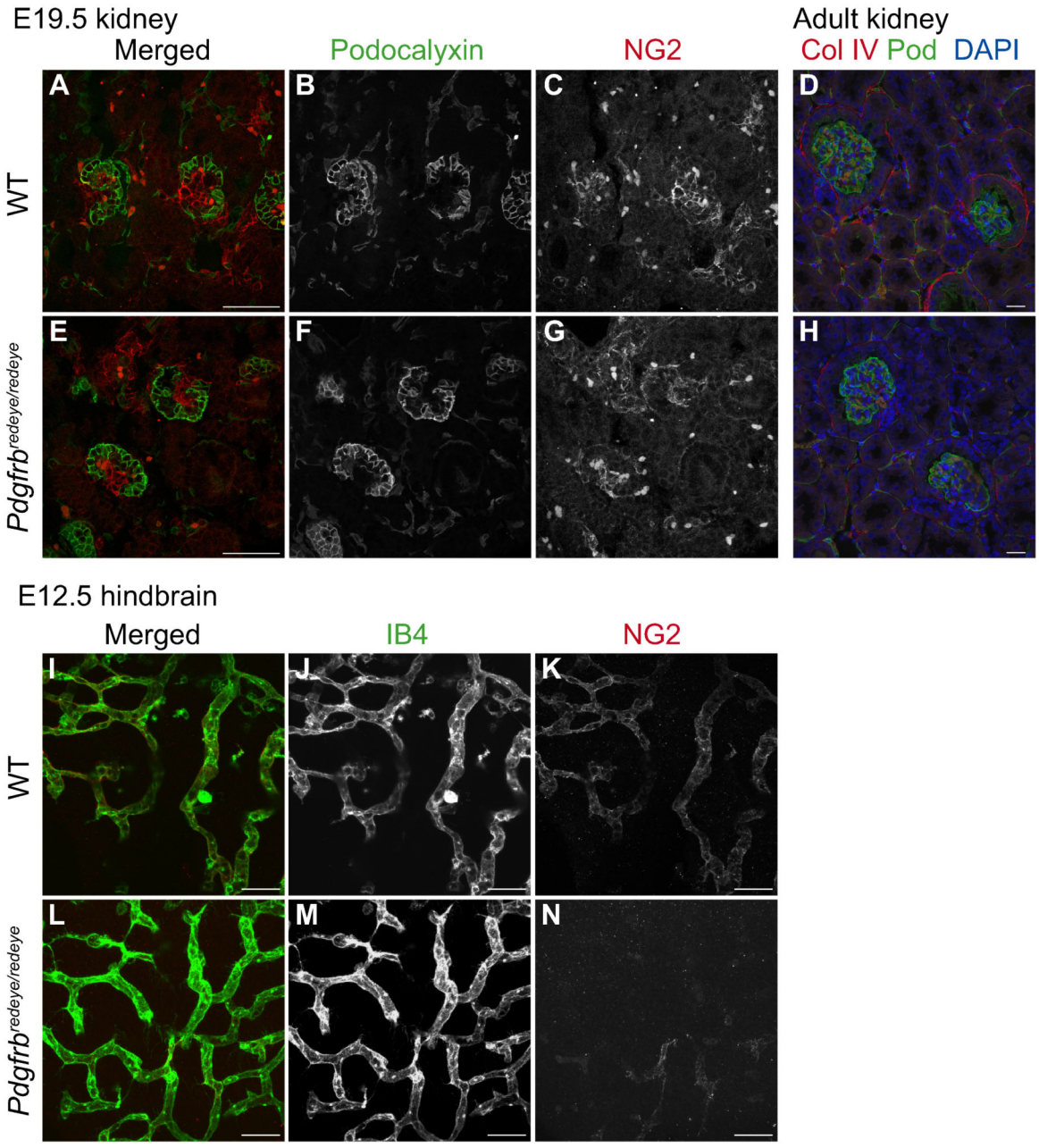

Figure 3. The pericyte recruitment deficiency is restricted to the CNS

The pericyte equivalent in the kidneys are mesangial cells which are recruited to the developing glomerulus at around E17.5. Paraffin sections of E17.5 WT (A-C) and *Pdgfrb*$^{redeye/redeye}$ kidneys (E-G) stained for podocytes with Podocalyxin (B, F) and mesangial cells with Proteoglycan NG2 (C, G) show similar numbers of mesangial cells being recruited. Paraffin sections of adult kidneys stained for vessels with Collagen IV and podocytes with Podocalyxin (Pod) also show normal histology (D, H). E12.5 embryonic hindbrains were also stained with IB4 for vessels (J, M) and NG2 for pericytes (K, N) in the developing CNS. WT hindbrains recruit pericytes normally (I-K) but *Pdgfrb*$^{redeye/redeye}$

hindbrains show decreased pericyte recruitment (L-N). Scale bars: 100 μm (D, H), 50 μm (all other images).

Europe PMC Funders Author Manuscripts

Europe PMC Funders Author Manuscripts

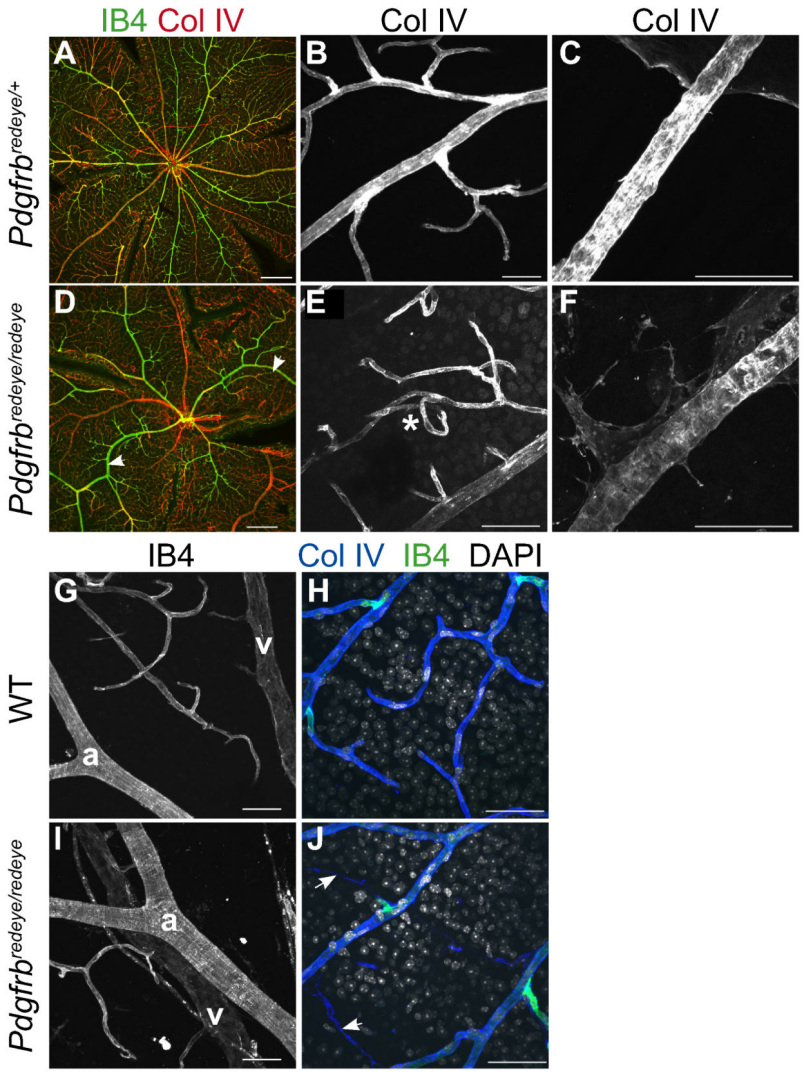

Figure 4. Loss of pericytes results in vascular patterning defects

Adult wholemount retinae stained with vessel markers IB4 and Collagen IV show regular patterning of vessels in a *Pdgfrb*$^{redeye/+}$ retina with straight vessels (A, B). In the *Pdgfrb*$^{redeye/redeye}$ retina the vessels are irregular and the arteries in particular seem not to extend straight towards the periphery (arrowheads, D). At higher magnification these vessels appear to be tortuous (asterisk, E). A Normal level of Collagen IV is expressed by pericytes as well as endothelial cells in *Pdgfrb*$^{redeye/+}$ retinae (C) and is decreased in *Pdgfrb*$^{redeye/redeye}$ retinae (F) arteries. WT retinae exhibit evenly spaced arteries (*a*) and veins (*v*) (G) but *Pdgfrb*$^{redeye/redeye}$ retinae show artery-vein crossover events (I) as well as acellular capillaries (arrows, J) that are characterised by positive Collagen IV staining and IB4 staining which are seen in WT retinae (H) but with the absence of nuclei, stained with DAPI. Scale bars: 200 μm (A, D), 50 μm (B, C, E-J).

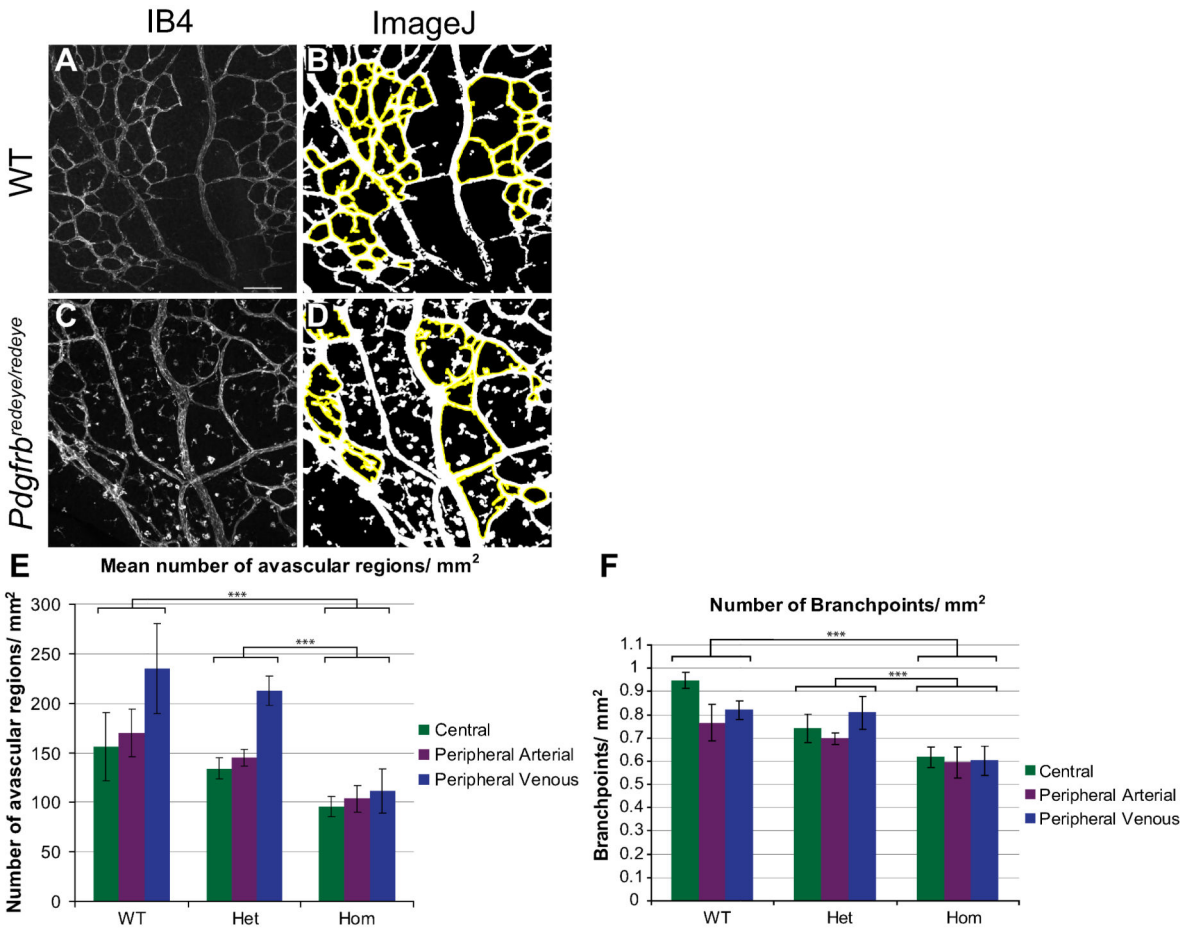

Figure 5. Vascular branching is defective in *Pdgfrb*$^{redeye/redeye}$ mutants

To characterise vessel patterning ImageJ software was used to quantify the avascular regions outlined in yellow (B, D) between vessels per mm^2 of P5 retinae (E). MetaMorph® software was used to quantify branchpoint number per mm^2 of P5 retinae (F). There are a greater number of smaller avascular regions and branchpoints (both central and peripheral) in WT and *Pdgfrb*$^{redeye/+}$ (Het) retinae than in *Pdgfrb*$^{redeye/redeye}$ (Hom) retinae (ANOVA $P <$ 0.001 in both cases, TukeyHSD ***$P < 0.001$) (E, F). Scale bars: 100 μm (A-D). Error bars: standard deviation of means.

Europe PMC Funders Author Manuscripts

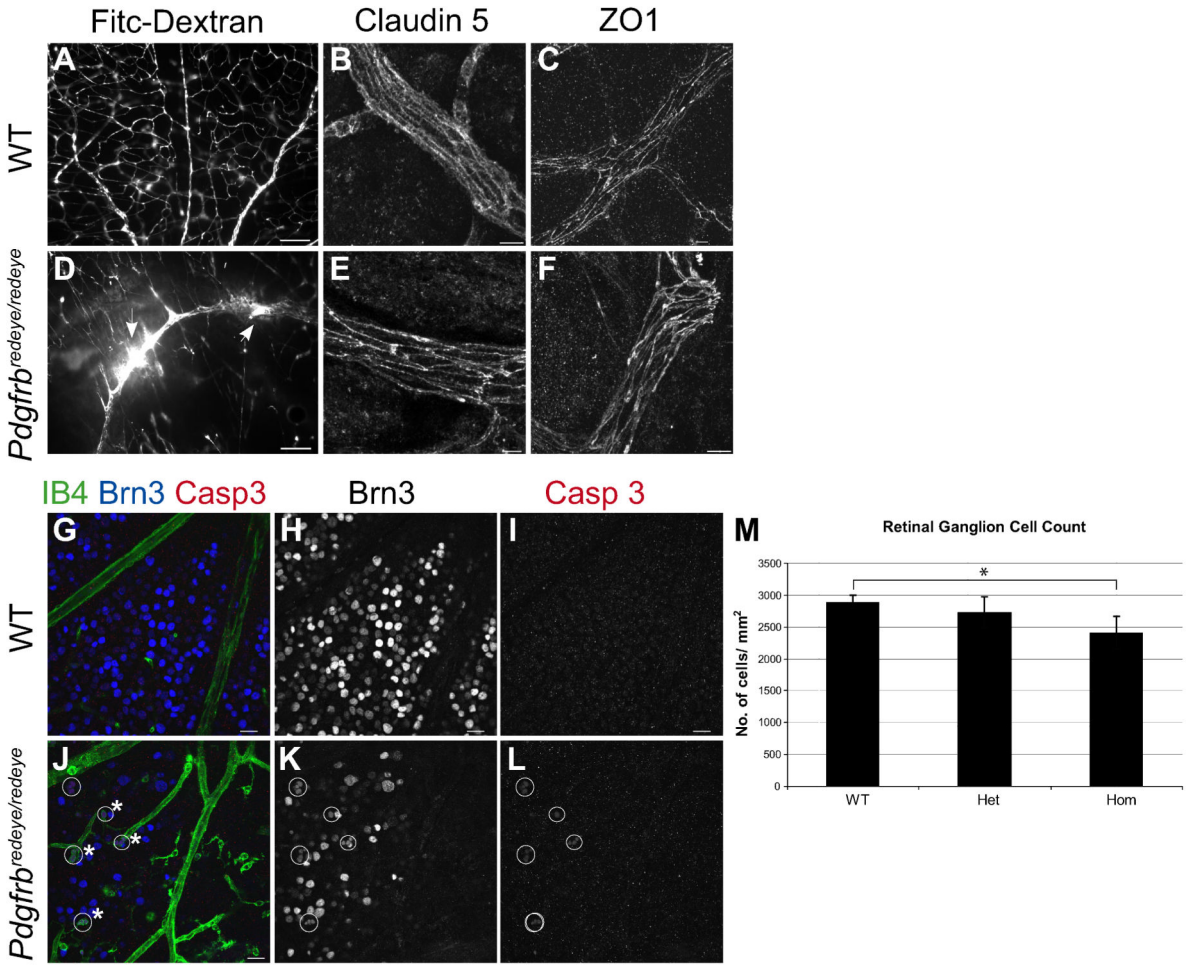

Figure 6. ***Pdgfrb*** $^{redeye/redeye}$ **mutants exhibit BRB dysfunction**

Vascular permeability was tested by intraperitoneal injection of 2kDa Fitc-Dextran at P10 which does not leak from WT vessels in the retina due to the BRB (A), but *Pdgfrb* $^{redeye/redeye}$ retinae exhibit vascular leakage (arrows, D). Claudin 5 and ZO1 are expressed in the tight junctions between endothelial cells in P5 WT (B, C) and *Pdgfrb* $^{redeye/redeye}$ mutants (E, F). To determine if BRB dysfunction causes neurodegeneration, P28 retinae were stained with IB4 (vessels and macrophages), Brn3 (RGCs) and the apoptosis marker Cleaved caspase 3 (Casp3) showing apoptotic RGCs (circles) being engulfed by macrophages in *Pdgfrb* $^{redeye/redeye}$ (asterisk, J) but not WT retinae (G). RGCs stained with Brn3 were counted in the centre of the retina in P28 WT (H), *Pdgfrb* $^{redeye/+}$ (Het) and *Pdgfrb* $^{redeye/redeye}$ (Hom) (K) animals. *Pdgfrb* $^{redeye/redeye}$ retinae had fewer ganglion cells than both WT and *Pdgfrb* $^{redeye/+}$ retinae (Kruskal-Wallis test $P = 0.002$, Mann-Whitney U-test $^{*}P < 0.05$) (K). Scale bars: 100 μm (A, D, G-L) and 10 μm (B, C, E, F). Error bars: standard deviation of the mean.